Left-Ventricle Global and Regional Functional Analysis from MDCT Images

Samuel Silva[1,2] and Beatriz Sousa Santos[1,2] and Joaquim Madeira[1,2]

[1]IEETA – Instituto de Engenharia Electrónica e Telemática de Aveiro
[2]Dep. Electrónica, Telecomunicações e Informática, Universidade de Aveiro

ABSTRACT

Left-ventricle functional analysis is of paramount importance for the assessment of coronary artery disease. Non-invasive coronary artery imaging using multiple-detector computed tomography (MDCT) provides a wealth of data concerning multiple cardiac phases. These have still to be explored in order to assess if further insight is possible regarding regional and functional analysis of the left ventricle leading to a more informed diagnosis and prognosis. Following on previous work regarding left-ventricle segmentation of all available cardiac phases in MDCT exams this article presents several parameters characterizing global and regional left ventricle function, computed for several cardiac phases and represented over time. Synchronized viewing of the different parameters is also supported.

1. Introduction

Left-ventricle functional analysis is of paramount importance for the assessment of coronary artery disease. Non-invasive coronary artery imaging is currently possible using MDCT scanners [PLLP06]. For this purpose the patient is injected with a contrast agent which improves the contrast of the heart chambers (atria and ventricles) and coronary arteries. Typically, the data provided by these exams consist in a set of 10 image volumes evenly distributed along the cardiac cycle. Each of these image volumes encompasses the full heart and therefore includes data concerning not only the coronary arteries but both atria and ventricles.

Scanner technology has been advancing at a fast pace and several studies have shown [FJO*07, WTY*08] that 64–MDCT imaging is clinically acceptable as a source to evaluate left ventricle (LV) function when compared to other image modalities such as cardiac magnetic resonance (CMR), echocardiography and single photon emission computed tomography (SPECT).

Apart from the work of Wesarg [Wes05], applied to CMR images, which explores several parameters (e.g., wall thickening and regional ejection fraction) and analysis methods (e.g., plots for regional mean values) over time, LV function analysis has been limited to computing global/regional data for the systolic and diastolic phases (e.g., Fischbach et al. [FJO*07], Okuyana et al. [OES*08] and Palazzuoli et al. [PCG*10]) not taking advantage of the cardiac data available in-between. Therefore, the question remains if further insight into LV function is possible if this additional data is considered. To answer this question, 1) LV data must be segmented for all cardiac phases; 2) different parameters deemed important to characterize global and regional LV function must be computed and presented and 3) these tools should be tested in clinical scenarios to assess their applicability.

The work reported here concerns step 2) and presents global and regional functional analysis of the LV from 4D MDCT cardiac images based on how different parameters characterizing LV function vary over time. The described features have been implemented in CardioAnalyzer [SMSSS10], a tool developed using Qt 4.5, MITK [MIT11] and ITK [ITK11].

This article starts with a brief description of the LV segmentation method and the representations used to depict the computed parameters followed by a description of the different parameters computed to characterize global and regional LV function. Finally, some conclusions and ideas for future work are presented.

2. Left ventricle segmentation

Prior to LV analysis, the endocardium and epicardium are identified using a semi-automatic segmentation method developed by the authors and implemented in CardioAnalyzer [SMSSS10].

Figure 1 shows different view planes depicting the endocardium (in red) and epicardium (in blue) for the end-systolic and end-diastolic phases. For easier processing the corresponding voxel masks encompassed by each contour are used (instead of the contour) and will be referred to as the endocardium and epicardium voxel masks. The myocardium is the region between the endocardium and the epicardium.

3. Data representation

To understand the analysis and representations presented along this article it is important to consider how the LV is

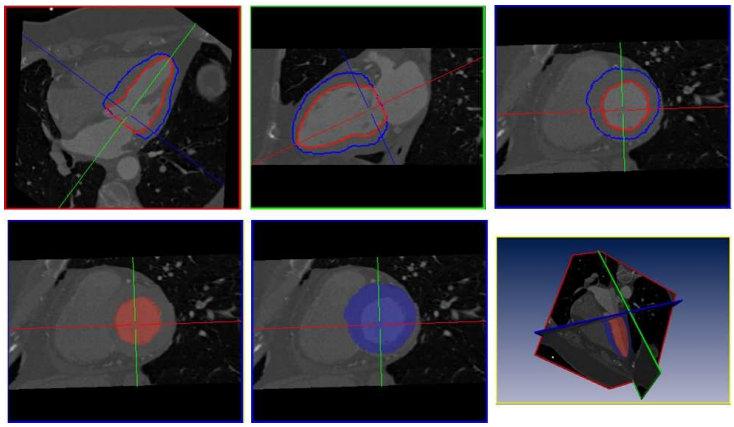

Figure 1: *Top, from left to right, four chambers, two chambers and short-axis views depicting the endocardium (red) and epicardium (blue) borders. Bottom, inner-endocardium voxel mask, inner-epicardium voxel mask and view plane positions in 3D.*

divided in different segments and how the data concerning each segment is usually represented.

The myocardium is usually divided in 17 segments used for analysis [CWD*02], by dividing the myocardium in three parts (annular tomographic regions) along its long axis (basal, mid-cavity and apical) and then dividing each of those parts in six, six and four angular segments respectively. A segment is included for the apical cap (not considered if the analysis is performed for the endocardium, i.e., the blood chamber). Each of these segments has a direct correspondence with the different regions of the polar map (also known as bull's-eye diagram) which is often used to depict myocardium analysis data (see figure 2).

4. Left Ventricle Global Analysis

The blood volumes for each cardiac phase are computed by counting the number of voxels in each segmented volume and multiplying by voxel volume according to image spacing. Having the blood volumes for all cardiac phases, it is possible to determine the end-systolic (lowest blood volume) and end-diastolic (highest blood volume) phases. Figure 3 shows line graphs depicting the blood volume for each cardiac phase (timepoints) for two patients. While in the first line graph the blood volume reaches a clear low at timepoint 2 (thus the end-systolic phase) in the bottom line graph the end-systolic phase is not as clearly apart from the neighbor phases.

The ejection fraction (EF) can then be computed as

$$EF = \frac{V_{ED} - V_{ES}}{V_{ED}}$$

where V_{ED} amd V_{ES} are the blood volumes for the end-diastolic and end-systolic phase respectively.

5. Left Ventricle Local and Regional Analysis

For LV regional analysis data concerning multiple LV regions is computed. Two different approaches are possible for regional analysis: one includes computing local data for the LV and another consists in computing data for each LV segment. In those situations where local measures are possible, both approaches can be used since an average value for each segment can be computed from the different local values available. For example, endocardium radius can be computed locally and a mean radius can be computed for each LV segment. On the other hand, some measures, e.g., blood volume, only make sense as a regional parameter. Furthermore, there are commonly used parameters, such as the systolic wall thickening (SWT) [KKM*09] which require the computation of local and regional values.

5.1. Regional Blood Volumes and Regional Ejection Fraction

Regional blood volumes are obtained by counting the number of voxels in each segment and then multiplying by voxel volume.

To assign the voxels to each segment, analysis is performed on short-axis slices. For each slice, the centroid of the voxel mask is computed and, for each voxel, the angle at which it is positioned relative to the horizontal (see Figure 5) is determined. The slice number is used to assign the voxel to a annular tomographic region (basal, mid-ventricular or apical) and set the correct number of segments expected in that region. Since segment numbering does not start at angle zero, an angle offset is also needed. A better alternative to the currently analysed voxel mask centroid is the corresponding centroid for the diastolic phase. This way, blood volumes are computed defining LV segments according to the LV long axis at rest.

By computing regional blood volumes for all available cardiac phases, it is possible to obtain an overview of their variation along the cardiac cycle. Figure 4 shows a line graph depicting several curves for the amount of blood found in each segment along the cardiac cycle.

A representation is also possible using a polar map for each cardiac phase depicting the regional blood volumes as shown in figure 6.

Regional ejection fraction is computed considering the regional blood volumes for the end-systolic phase and the corresponding regional blood volumes determined for the diastolic phase. The polar maps in figure 7 depict the regional ejection fraction for an healthy patient (left) and for a patient with diagnosed low myocardium contractility (right).

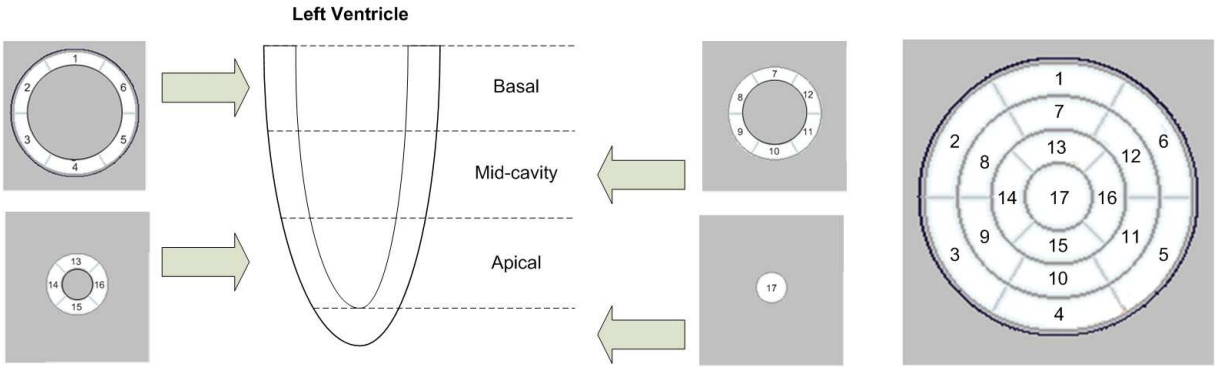

Figure 2: *Segments considered by physicians when analysing the left ventricle and their placement in the polar map [CWD*02].*

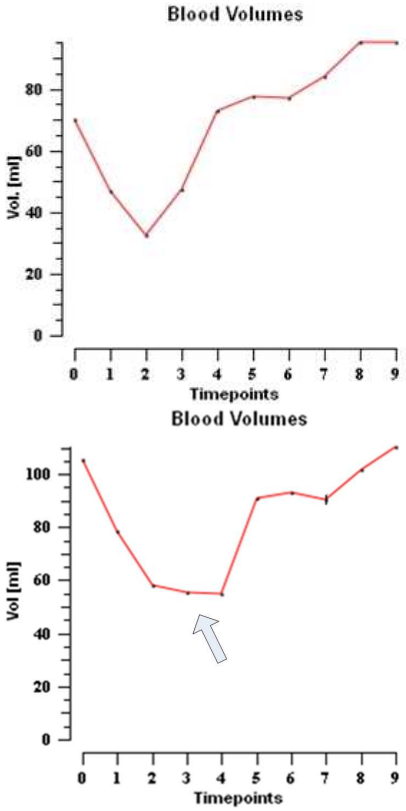

Figure 3: *Left ventricle global analysis showing blood volumes for each cardiac phase for two patients. Notice that the bottom line graph exhibits a rather difficult to identify end-systolic phase.*

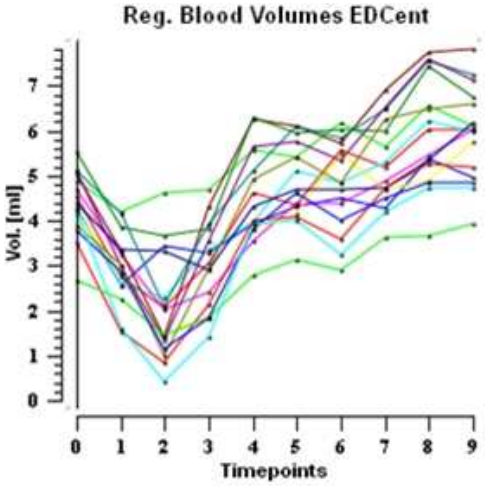

Figure 4: *Regional blood volumes graph.*

Notice the very clear prevalence of red in the second polar map, evidence of very low regional ejection fractions.

5.2. Endocardium Radius

Given an endocardium segmentation it is possible to compute its radius and, by analysing how it changes along the cardiac cycle, obtain data regarding how the myocardium contracts.

For each short-axis slice the endocardium centroid is obtained and the radius is computed at constant angular intervals (see figure 8). A trade-off between the number of angular steps and computation speed is performed considering that the endocardium is not prone to present abrupt changes. The data presented in this article has been computed using 25 angular steps per slice. The image is traveled along each angular direction looking for the border of the endocarium voxel mask. Then, the radius is converted from image units to world units considering image spacing

$$R(mm) = \sqrt{((v_x - c_x) \times s_x)^2 + ((v_y - c_y) \times s_y)^2}$$

where (c_x, c_y) are the centroid coordinates, (v_x, v_y) are the border voxel coordinates and s_x and s_y concern image spacing as depicted in figure 8. Even though the segmentation method includes a hole filling step and all the segmentations are supervised there is always the chance of a "hole" in the mask. To avoid a badly computed radius, when what is thought to be a border voxel is reached the image keeps being traveled in the same direction for some additional voxels. If an active voxel is found the algorithm goes back to looking for a border voxel. Otherwise, the border voxel initially found is considered.

Using the endocardium centroids computed for each short-axis slice might not give a proper idea concerning radius variation assymetry. This is due to the fact that the reference point (centroid) is always computed from the currently analysed slice. Therefore, it does not provide a global reference to be used for all phases. In order to explore radius assymetries, the centroids for the diastolic phase are used to

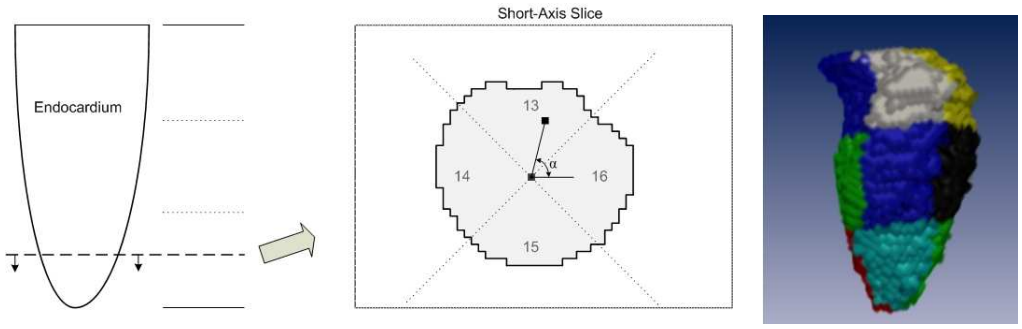

Figure 5: *Assigning each voxel in the endocardium voxel mask to a LV segment: each short-axis slice is processed; the slice number and the angle computed for each voxel determines its segment. Right, the endocardium voxel mask shown with segments in different colors (partial view).*

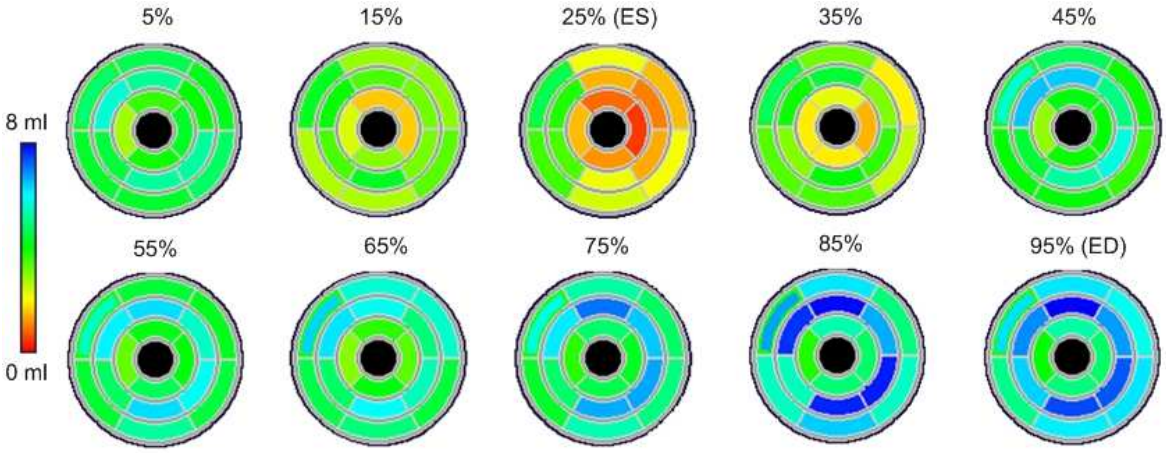

Figure 6: *Regional blood volumes for each available cardiac phase. End-systolic (ES) and end-diastolic (ED) phases defined according to total blood volumes.*

compute endocardium radii for all cardiac phases, thus considering the LV long-axis at rest.

Figure 10 shows the polar maps for endocardium radius using, on top, each phase centroids and, on the bottom, diastolic phase centroids. Notice how on the bottom polar maps it is possible to see some radius assimetry (smaller radius on the right side of the polar map) in the end-sistolic (ES) phase.

Figure 11 shows the mean segmental endocardium radius values over the different cardiac phases. In order to allow an easier analysis the user can choose to view only the curves associated with each annular tomographic region (apical, mid-ventricular or basal segments) or any combination of the three.

5.2.1. Endocardium Radius Variation

Given the shape of the endocardium, the radius is larger in the basal region and smaller in the apical region. Therefore, when representing the computed radius in a polar map using, for example, a rainbow color scale, the apical region will always limit the perception of how the radius varies on the remaining regions. One alternative would be to represent radius variation (regarding the corresponding radius in the diastolic phase) but this would result in a similar problem with the basal region, where radius variation is higher, hindering the analysis of the apical region. Thus, radius variation is expressed as a percentage of the corresponding radius in the diastolic phase which results in a normalization of the variation for all regions.

Comparing the end-systolic polar maps in figures 10 and 9, drawn for the same exam data, it is clear that representing the radius variation better highlights segments (on the left of the polar map) with smaller variation while leaving the remaining segments with an homogeneous color.

5.3. Myocardium Thickness

To compute myocardium thickness, myocardium voxel mask is obtained by subtracting the endocardium voxel mask from the epicardium voxel mask. Myocardiun thickness is computed using a similar method as the one described for endocardium radius computation. Each short-axis slice is analyzed and, using the corresponding end-diastolic phase centroid, myocardium thickness is computed at constant angular steps.

Having myocardium wall thicknesses, systolic wall thickening (SWT) [KKM*09] can be computed as

$$SWT = 100 \times \frac{WT_{ES} - WT_{ED}}{WT_{ES}}$$

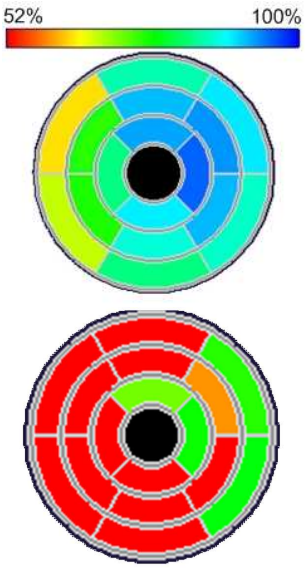

Figure 7: *Regional ejection fraction. Top, polar map for healthy patient. Bottom, polar map for patient with depressed ejection fraction.*

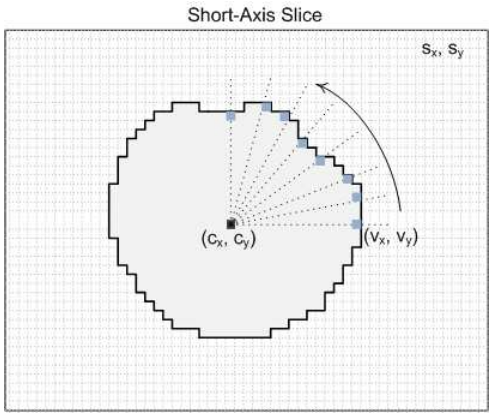

Figure 8: *Endocardium radius computation. Each short-axis image is traveled along different directions looking for border voxels.* (c_x, c_y)*: centroid coordinates;* (v_x, v_y)*: border voxel coordinates;* s_x*,* s_y*: image spacing.*

where WT_{ES} and WT_{ED} are the wall thickness for the end-systolic and end-diastolic cardiac phases.

6. Further Visualization Options

All the described parameters can been analysed in parallel (figure 12) and therefore several features are required which allow synchronized viewing of the different polar maps and line graphs.

When a cardiac phase is selected, for all parameters the corresponding polar map is shown and a vertical line is presented in each line graph as seen in figure 12.

When a segment in the polar map is selected, it is automatically selected in all polar maps and the corresponding curve, in each line graph, is also highlighted. Furthermore, the anatomical region associated with the segment is highlighted over the image data. Figure 13 shows a polar map with segment 10 selected, the corresponding line graph with the highlighted curve and a short-axis and two-chambers view of the LV with the highlighted region.

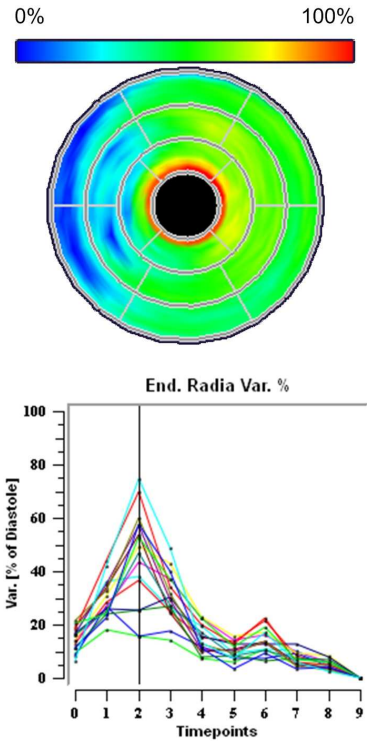

Figure 9: *Polar maps depicting endocardium radius variation for the end-systolic phase and segmental mean radius variation curves.*

7. Conclusions

This article presents different parameters characterizing global and regional LV function computed from 4D MDCT images of the heart. The computed data is represented using line graphs presenting mean segmental values along time and synchronized polar maps depicting a colored representation for each cardiac phase.

The different parameters allow a characterization of various aspects of LV cardiac function and several interesting outcomes can be highlighted. Notice, for example, how the curves for endocardium radius or regional blood volumes over time follow a common pattern (with different offset between annular tomographic regions as seen in figure 11). If one of the segmental curves stands out it might be due to a segmental problem (see line graph in figure 13). Notice also how in figure 3 the curve on the bottom line graph shows a different behavior around the end-systolic phase which would not be clear if only a global parameter such as the ejection fraction was used. Furthermore, providing a "connection" to the anatomical region associated with the different segments allows quickly checking the anatomy to, for example, rule out abnormal parameters due to a segmentation problem.

Informal evaluation of the presented features has been carried out with the help of a physician with daily experience in

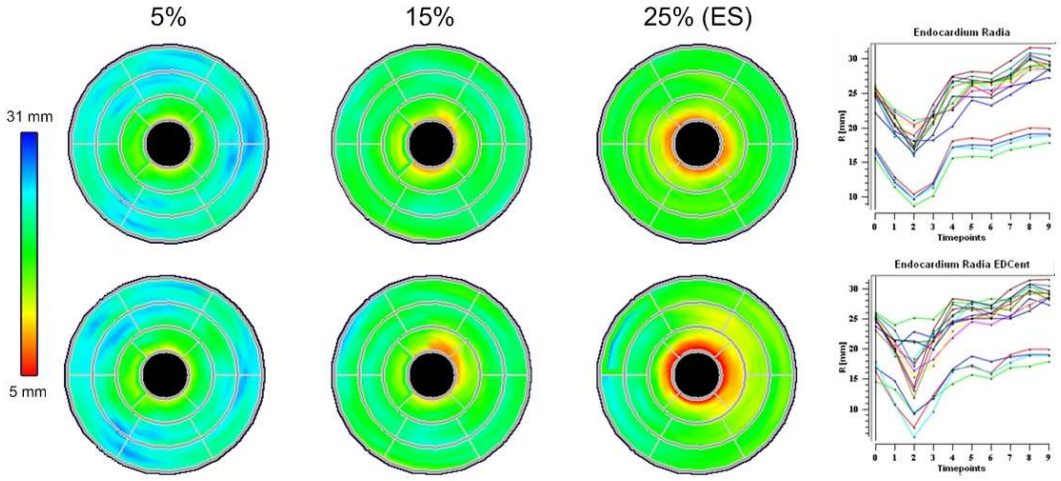

Figure 10: *Polar maps depicting endocardium radius for different cardiac phases. Top, endocardium radius has been computed using the centroids for each cardiac phase; bottom: endocardium radius has been computed using the diastolic phase centroids for all phases. Notice how the line graphs on the right present noticeable differences, particularly around the end-systolic phase (timepoint 2).*

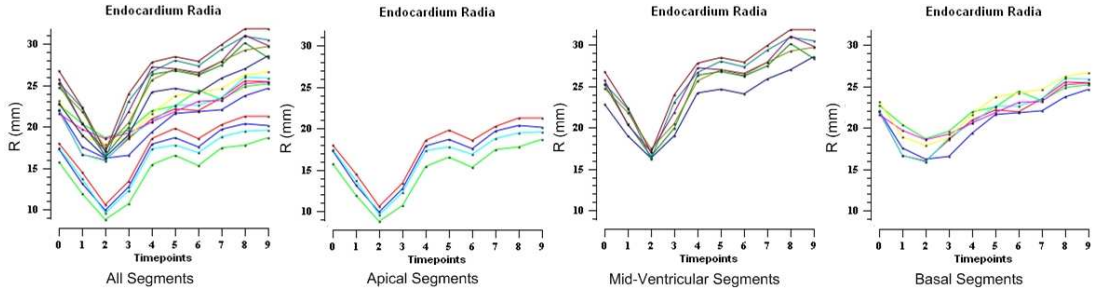

Figure 11: *Line graphs showing the evolution of segmental mean endocardium radius along the cardiac cycle. Apical, mid-ventricular and basal segmental curves can be viewed separately.*

cardiac image analysis. He regards the provided features, in particular myocardium thickness, potentially important for diagnosis, since they provide indication of possible infarction regions. Myocardium thickness might also be advantageous when combined with perfusion assessment data.

Creating a polygonal mesh is also possible from the endocardium and epicardium masks using, for example, the well known marching cubes argorithm [LC87]. In fact, we already have such a feature to allow a visual analysis of the endocardium/epicardium. These meshes can be used as an alternative support to represent the computed parameters but it is important to notice that a 3D model does not offer a "whole ventricle view" as the one provided by the polar map and, besides, the latter is well known by users.

Our next goal is to perform clinical validation to assess how the different polar maps and line graphs can help during analysis and diagnosis. This requires that knowledge concerning LV physiology is used to interpret the different polar maps and line graphs.

Another interesting route for future work it to study how regional functional analysis of the LV can be related with myocardial perfusion assessment. Preliminary work concerning myocardial perfusion assessment from adesonise-induced stress MDCT as been presented by the authors in [SBL*11].

Aknowledgements

The first author is supported by grant SFRH/BD/38073/2007 awarded by the Portuguese Science Foundation (FCT).

References

[CWD*02] CERQUEIRA M. D., WEISSMN N. J., DILSIZIAN V., JACOBS A. K., KAUL S., LASKEY W. K., PENNEL D. J., RUMBERGER J. A., RYAN T., VERANI M. S.: Standardized myocardial segmentation and nomenclature for tomographic imaging of the heart: A statement for healthcare professional from the cardiac imaging comitee of the council on clinical cardiology of the american heart association. *Circulation 105* (2002), 539–542.

[FJO*07] FISCHBACH R., JUERGENS K., OZGUN M., MAINTZ D., GRUDE M., SEIFARTH H., HEINDEL W., WICHTER T.: Assessment of regional left ventricular function with multidetector-row computed tomography versus magnetic resonance imaging. *European Radiology 17*, 4 (2007), 1009–1017.

[ITK11] ITK: Insight segmentation and registration toolkit. http://www.itk.org/ ((online Mar 2011)).

[KKM*09] KRISTENSEN T., KOFOED K., MOLLER D., ERSBOLL M., KÜHL T., RECKE P., KOBER L., NIELSEN M., KELBAEK H.: Quantitative assessment of left ventricular systolic

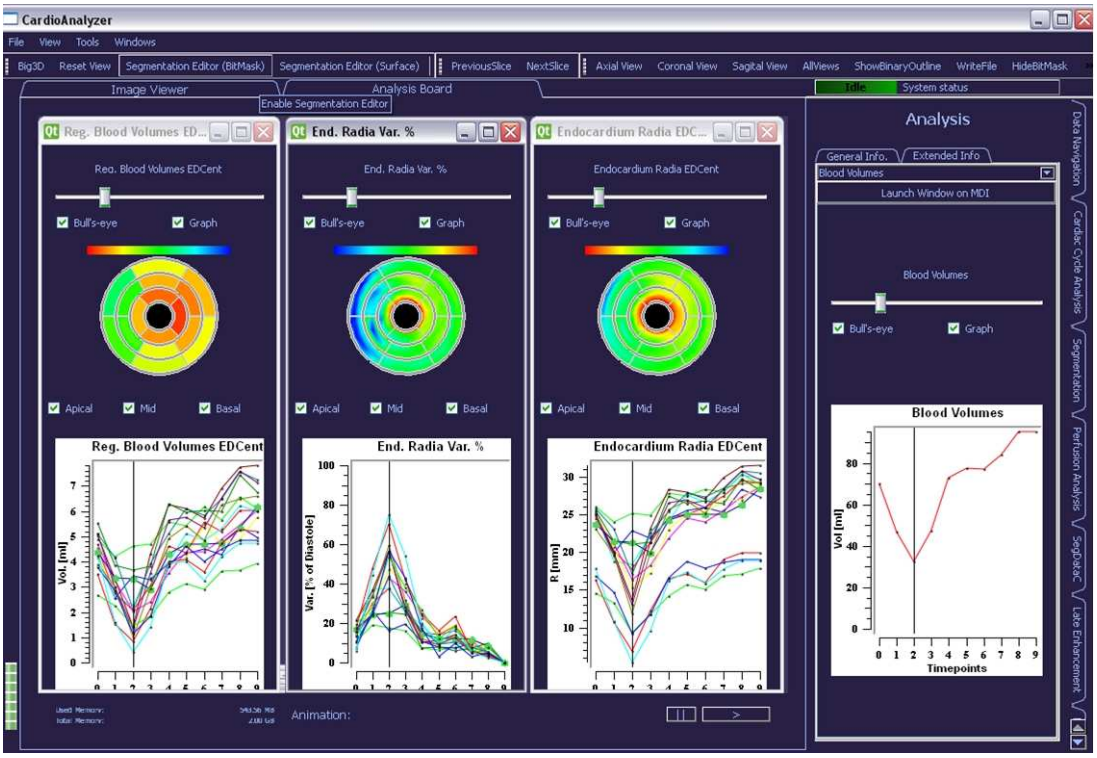

Figure 12: *Screenshot of CardioAnalyzer showing several analysis windows. All representations are synchronized.*

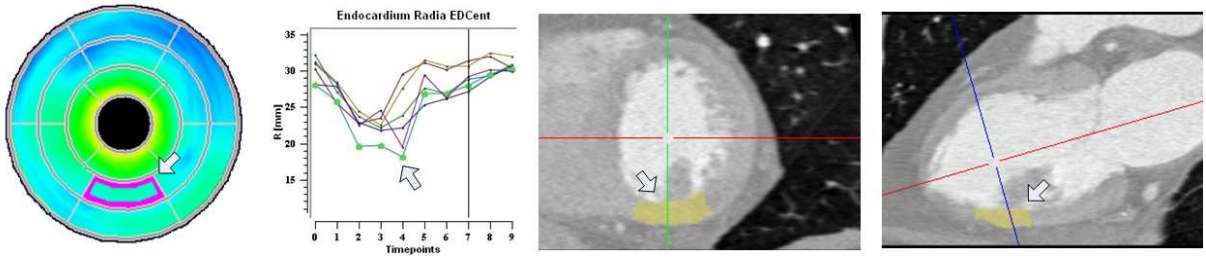

Figure 13: *Selecting a segment in a polar map representation: all polar maps will show the selection, all line graphs will have the corresponding curve highlighted and the anatomical region is depicted over the LV image.*

wall thickening using multidetector computed tomography. *European Journal of Radiology 72*, 1 (2009), 92–97.

[LC87] LORENSEN W. E., CLINE H. E.: Marching cubes: A high resolution 3D surface construction algorithm. *SIGGRAPH Comput. Graph. 21* (August 1987), 163–169.

[MIT11] MITK: Medical imaging interaction toolkit. http://www.mitk.org ((online Mar 2011)).

[OES*08] OKUYAMA T., EHARA S., SHIRAI N., SUGIOKA K., OGAWA K., OE H., KITAMURA H., ITOH T., OTANI K., MATSUOKA T., INOUE Y., UEDA M., HOZUMI T., YOSHIYAMA M.: Usefulness of three-dimensional automated quantification of left ventricular mass, volume, and function by 64-slice computed tomography. *Journal of Cardiology 52*, 3 (2008), 76–284.

[PCG*10] PALAZZUOLI A., CADEMARTIRI F., GELEIJNSE M., MEIJBOOM B., PUGLIESE F., SOLIMAN O., CALABRÓ A., NUTI R., FEYTER P.: Left ventricular remodelling and systolic function measurement with 64 multi-slice computed tomography versus second harmonic echocardiography in patients with coronary artery disease: A double blind study. *European Journal of Radiology 73*, 1 (2010), 82–88.

[PLLP06] PONS-LLADÓ G., LETA-PETRACCA R.: *Atlas of Non-Invasive Coronary Angiography by Multidetector Computed Tomography*. Springer, 2006.

[SBL*11] SILVA S., BETTENCOURT N., LEITE D., ROCHA J., CARVALHO M., MADEIRA J., SOUSA SANTOS B.: Myocardial perfusion analysis from adenosine-induced stress MDCT. In *Proc. Iberian Conference on Pattern Recognition and Image Analysis (IbPRIA 2011) (to appear)* (Las Palmas de Gran Canaria, Spain, 2011).

[SMSSS10] SILVA S., MADEIRA J., SOUSA SANTOS B., SILVA A.: Cardioanalyser: A software tool for segmentation and analysis of the left ventricle from 4D MDCT images of the heart. In *Proc. 7th International Conference on Biomedical Visualisation (MediVis'10)* (London, UK, 2010), pp. 629–634.

[Wes05] WESARG S.: AHA conform analysis of myocardial function using and extending the toolkits ITK and VTK. In *Computer Assisted Radiology and Surgery (CARS 2005), International Congress Series* (2005), vol. 1281, pp. 44–49.

[WTY*08] WU Y.-W., TADAMURA E., YAMAMURO M., KANAO S., OKAYAMA S., OZASA N., TOMA M., KIMURA T., KOMEDA M., TOGASHI K.: Estimation of global and regional cardiac function using 64-slice computed tomography: A comparison study with echocardiography, gated-spect and cardiovascular magnetic resonance. *International Journal of Cardiology 128*, 1 (2008), 69–76.